

# Topological network alignment uncovers biological function and phylogeny

Oleksii Kuchaiev<sup>z</sup>, Tijana Milenković<sup>z</sup>, Vesna Memišević,  
Wayne Hayes, Nataša Pržulj

Department of Computer Science, University of California, Irvine, CA 92697-3435, USA

<sup>z</sup>These authors contributed equally to this work

To whom correspondence should be addressed; E-mail: natasha@ics.uci.edu.

**Sequence comparison and alignment has had an enormous impact on our understanding of evolution, biology, and disease. Comparison and alignment of biological networks will likely have a similar impact. Existing network alignments use information external to the networks, such as sequence, because no good algorithm for purely topological alignment has yet been devised. In this paper, we present by far the most complete topological alignments of biological networks to date. We demonstrate that both species phylogeny and detailed biological function of individual proteins can be extracted from a solely topological comparison of networks. Topological alignments provide an independent new source of phylogenetic information. Our alignment of the protein-protein interaction networks of two very different species—yeast and human—indicate that even distant species share a surprising amount of network topology with each other, suggesting broad similarities in internal cellular wiring across all life on Earth.**

A network (or graph) is a collection of nodes (or vertices), and connections between them called edges. Network alignment<sup>1</sup> is the problem of finding similarities between the structure or topology of two or more networks. Exactly analogous to sequence alignment, network alignments are useful because we may know a lot about some of the nodes in one network and almost nothing about nodes in the other that share a similar topology; then, specialized knowledge about one may tell us something new about the other. Network alignments can also be used to measure the global similarity between complete networks of different species. Given

a group of such biological networks, the matrix of pairwise network similarities between them can be used to infer phylogenetic relationships.

Analogous to sequence alignments, there exist *local* and *global* network alignments. Thus far, the majority of methods have focused on local network alignments.<sup>2-5</sup> With local alignments, mappings are chosen independently for each local region of similarity, revealing similarity between pathways or small complexes. However, local alignments can be ambiguous, with one node having different pairings in different local alignments. In contrast, a global network alignment provides a unique alignment between every node in the smaller network and exactly one node in the larger network, even though this may lead to imperfect matchings in some local regions. Local network alignments are generally not able to identify large subgraphs that have been conserved during evolution.<sup>2,3</sup> Global network alignment has been studied previously,<sup>6,7</sup> but most existing methods incorporate some *a priori* information about nodes such as sequence similarities of proteins in PPI networks,<sup>7</sup> or they use some form of learning on a set of “true alignments”.<sup>6</sup> In contrast, our alignments are based *solely* on topological information and do not require learning. Our new topology-based network alignment tool is called GRAAL (GRAPh ALigner).

Using GRAAL, we align the human PPI network of Radivojac et al.<sup>8</sup> to the Collins et al. yeast PPI network,<sup>9</sup> which we call “human1” and “yeast2”, respectively. We chose yeast as our second species because currently it has a high quality PPI network, with 16,127 interactions (edges) among 2,390 proteins (nodes). GRAAL aligns 1,623 of the edges in yeast2 (10.06% of them) to edges in human1. We call the 10.06% the *edge correctness*. There are 858 nodes involved in these “correct” edge alignments, representing 36% of all yeast2 nodes. We obtained similar edge correctness scores for other alignments of yeast<sup>9,10</sup> and human<sup>10-12</sup> (Supplementary Figure 7). In addition to counting aligned edges, it is important that the aligned edges cluster together to form large and dense connected subgraphs, in order to uncover such regions of similar topology. We define a *common connected subgraph* (CCS) as a connected subgraph (not necessarily induced) that appears in both networks. Our largest CCS (Figure 1A) has 1,001 interactions amongst 290 proteins, which comprises 12.1% of the proteins in the yeast2 network. The second largest CCS has 157 interactions amongst 29 nodes, depicted in Figure 1B. The entire common subgraph is presented in Supplementary Figure 8.

GRAAL uncovers common connected subgraphs (CCSs) that are substantially larger than those produced by currently published algorithms. The best currently published global alignment of similar networks is the alignment of yeast and fly by ISORANK,<sup>7</sup> which uses sequence information in addition to topological information. It aligns 1,420 edges, but its largest CCS contains just 35 nodes and 35 edges. Despite the fact that human is more similar to fly than yeast (human and fly are in the kingdom Animalia while yeast is in Fungi), our largest CCS aligns 28 times as many edges and 8.3 times as many nodes. Our *second* largest CCS has a similar number of nodes to ISORANK’s *largest*, but is 4.5 times as dense in terms of edges. Furthermore, we applied ISORANK to our yeast2-human1 data using only topological information. We found that it aligns 628 interactions (giving an edge correctness of only 3.89%), with its largest CCS having just 261 interactions among 116 proteins. Another popular global network

alignment method is Graemlin.<sup>6</sup> In addition to topology, this method requires a variety of other input information, including phylogenetic relationships between the species being aligned. In contrast, GRAAL's *output* can be used to infer phylogenetic relationships.

Judging the quality of GRAAL's alignment against a random alignment of yeast2-human1, we find a p-value of at most  $7 \times 10^{-8}$ , indicating that it is a high-quality alignment. Given that this alignment is a good one, we also find that the amount of network similarity between yeast2 and human1 is higher than one would expect between two random networks, having a p-value of at most 0.05 (using the most appropriate available null model; see the Methods section). This tells us that yeast and human, two very distant species, enjoy a significant amount of network similarity. In terms of the biological significance of our alignment, we find the following. (i) That 42.43%, 12.5%, 4.56%, 1.73%, and 0.55% of aligned protein pairs share at least one, two, three, four, and five GO terms, respectively, with p-values in the  $10^{-2}$  to  $10^{-3}$  range. (ii) GRAAL identifies conserved functional modules across species, with Figure 1B depicting a good example. (iii) From the list of yeast mitochondria-related genes associated with defects in growth on non-fermentable substrates that have human orthologs involved in mitochondrial disease,<sup>13</sup> GRAAL successfully aligns 30% of such yeast proteins to human mitochondrial disease genes, with a p-value of  $10^{-4}$ . For example, yeast SDH1 and SDH2 proteins are aligned to human MMAA and MUT proteins, respectively, that are involved in methylmalonic acidemia.<sup>13-15</sup> Additionally, yeast PDB1 protein is aligned to human MDH2 protein, a mitochondrial protein responsible for energy generation that is down-expressed in the presence of ulcerative colitis and therefore implicated in its pathogenesis.<sup>16</sup> Thus, our method recognizes solely from network topology the biological signal that has previously been demonstrated by orthology relationships from sequence analysis. (iv) GRAAL pairs human cancer proteins with yeast proteins whose orthologs in human are involved in cancer. In particular, we considered as cancer genes those genes involved in cancer pathways according to NetPath<sup>1</sup>. Examples of aligned cancer protein pairs include human TP53 protein to yeast RPS13 protein, human MAPK3 protein to yeast RPL30 protein, and human TRAF6 protein to yeast YAP1 protein, respectively. Additionally, human UPK1A and KCNJ8 proteins that are directly or indirectly characterized as being involved in cancer in the literature<sup>17-19</sup> are aligned to yeast proteins MCM7 and CDC27, respectively, whose human orthologs are involved in cancer pathways in NetPath.

With the above validations in hand, we believe that GRAAL's alignments can be used to predict biological characteristics of un-annotated proteins based on their alignments with annotated ones. Of the 2,390 protein pairs in our yeast2-human1 alignment, we identify 36 un-annotated human proteins whose aligned yeast proteins are annotated, and 228 un-annotated yeast proteins whose aligned human proteins are annotated. Predictions from the alignment are presented in Supplementary Tables 4 and 5. Some of these predictions are supported in the literature, while we found none that are contradicted. For example, of the 36 un-annotated human proteins, we found 28 discussed in the literature; for 11 of those 28 proteins (39%) a function consistent with our prediction was mentioned, while the remaining 17 were neither corroborated nor con-

---

<sup>1</sup><http://www.netpath.org/>

tradicted. We present our literature-validated predictions for these 11 human proteins in Table 1.

Continuing our alignment-based predictions now with yeast, we start with 228 un-annotated yeast proteins for which the aligned human proteins are annotated (Supplementary Table 5). We attempted manual literature validation of only those 124 pairs with topological similarity of 95% or greater, since we consider these our most confident predictions. Of these 124, we were able to find literature or SGD<sup>20</sup> discussions of their function in 96 cases; of those 96, there were 16 (17%) that explicitly mention functions consistent with our predictions, while the remainder were neither corroborated nor contradicted. For example, we predict that yeast protein RMD9 has cytokine activity, i.e., that it controls the survival, growth, differentiation and effector function of tissues and cells; we also predict its involvement in growth factor; SGD<sup>20</sup> describes it as the mitochondrial protein required for respiratory growth. For yeast proteins ERV46 and ERP5, we predict transporter activity; SGD confirms that they are involved in ER to Golgi transport. We predict that yeast protein FAP1 is involved in transcription; SGD and Green *et. al.*<sup>21</sup> associate it with transcription factor activity. We predict that yeast protein SNA2 is involved in ion, sodium ion, and calcium ion transport; SGD characterizes it as being involved in cation transport. Finally, for yeast proteins TEX1 and UPF3, we predict transcription factor activity; both SGD and Garcia *et. al.*<sup>22</sup> describe TEX1 as being involved in mRNA export and being the component of the transcription export (TREX) complex; similarly, the loss of UPF3 gene function has been shown to cause global changes in the yeast transcriptome.<sup>23</sup> For the remaining validations for yeast, see the Supplementary Information. Note that, since most proteins perform multiple functions, and since indications on biological function of un-annotated proteins in the literature are limited, it is likely that more than 39% and 17% of our predictions for human and yeast proteins are correct, respectively. Note also that not all functions that occur in human have meaning in yeast, so the lower “hit rate” in yeast is not surprising. In addition to manual literature validation, we attempted to validate computationally all of our predictions for yeast using the literature search and text mining tool CiteXplorer.<sup>24</sup> For 87 out of 228 yeast proteins (38.1%), this tool found at least one article mentioning the protein of interest in the context of at least one of our predictions for the protein.

We believe that none of our validated network-based predictions of human protein function could have been predicted using sequence comparison, because the sequences do not share nearly enough identity. In particular, the average sequence identity across validated, network-aligned pairs was only 5.7% with a maximum of 9.8%, which is comparable to the sequence identity found between two randomly chosen proteins.<sup>25</sup> Thus, PPI network topology provides a novel, independent method for function prediction, with value over and above sequence-based methods.

Finally, we describe a completely different application: how purely topological alignment of metabolic networks obtained by GRAAL can be used to recover phylogenetic relationships. Although related attempts exist,<sup>26</sup> they use sequence similarity to align protein pairs between networks. Since we use network topology to define protein similarity, our information source is fundamentally different. Thus, our algorithm recovers phylogenetic relationships (but currently

not the evolutionary timescale of species divergence) in a completely novel and independent way from all existing methods for phylogenetic recovery.

It has been shown that PPI network structure has subtle effects on the evolution of proteins and that reasonable phylogenetic inference can only be done between closely related species.<sup>27</sup> In the KEGG pathway database, there are 17 Eucaryotic organisms with fully sequenced genomes,<sup>28</sup> of which seven are protists, six are fungi, two are plants, and two are animals. Here we focus on protists (see Supplementary Information for fungi). For each organism, we extract the union of all metabolic pathways from KEGG, and then find all-to-all pairwise network alignments between species using GRAAL. The edge correctness scores between pairs of protist networks range from 25% to 80%. We create phylogenetic trees using the nearest distance algorithm,<sup>2</sup> with pairwise edge correctness as the distance measure. We compare our phylogenetic trees to the published ones<sup>3</sup> that are obtained from genetic or amino acid sequence alignments.<sup>29,30</sup> Figure 2 presents our phylogenetic tree for protists and shows that it is very similar to that found by sequence comparison.<sup>29</sup> We can estimate the statistical significance of our tree by measuring how it compares to trees built from random metabolic networks; we find that the p-value of our tree is less than  $10^{-3}$ . We also find that the topologies of the entire metabolic networks of *Cryptosporidium parvum* and *Cryptosporidium hominis* are very similar, having edge correctness of 71.5%. This result is encouraging since these organisms are two morphologically identical species of Apicomplexan protozoa with 97% genetic sequence identity, but with strikingly different hosts<sup>31</sup> that contribute to their divergence.<sup>32</sup>

The fact that we recover almost the same tree as sequence-based methods is both a strong validation of our method, and a novel, independent verification of the sequence-based phylogeny. Given that our phylogenetic tree is slightly different from that produced by sequence, there is no reason to believe that the sequence-based one should *a priori* be considered the correct one. Sequence-based phylogenetic trees are built based on multiple alignment of gene sequences and whole genome alignments. Multiple alignments can be misleading due to gene rearrangements, inversions, transpositions, and translocations that occur at the substring level. Furthermore, different species might have an unequal number of genes. Whole genome phylogenetic analyses can also be misleading due to non-contiguous copies of a gene or non-decisive gene order.<sup>33</sup> Our tree suffers none of these problems. It does not depend on our current technical ability to process strings of genetic code. Instead, it lets biology do the processing for us, and then directly uses gene products—proteins, enzymes, and the interactions between them. The largest caveat is the noise currently existing in the data representing these interaction networks.

Network alignment has applications across an enormous span of domains, from social networks to software call graphs. In the biological domain, the mass of currently available network data will only continue to increase. We believe that high-quality topological alignments can yield new and pivotal insights into function, evolution, and disease.

---

<sup>2</sup><http://www.mathworks.com/access/helpdesk/help/toolbox/bioinfo/index.html>

<sup>3</sup><http://fungal.genome.duke.edu/>

## Methods

For our purposes, an alignment of two networks  $G$  and  $H$  consists of a set of ordered pairs  $(u;v)$ , where  $u$  is a node in  $G$  and  $v$  is a node in  $H$ ; a “good” alignment is one in which the neighborhoods of  $u$  and  $v$  are as topologically similar as possible, across all the aligned pairs  $(u;v)$ . (See the Supplementary Information for details.)

Even if two networks are identical, they can be “drawn” in a myriad of different ways. Thus, their identity may not be obvious, and in fact no efficient method is known for finding an isomorphism between them. In the real world, networks are rarely even of the same size, much less identical, and so the problem of alignment becomes more ambiguous. Biological networks also contain copious noise, including both missing and false edges, further complicating the problem.

Our algorithm, GRAAL (details in the Supplementary Information), incorporates facets of both local and global alignment. We match pairs of nodes originating in different networks based on a highly constraining measure of their “local topological similarity”, as defined by Milenković and Pržulj.<sup>34</sup> We align each node in the smaller network to exactly one node in the larger network. The matching proceeds using a technique analogous to the “seed and extend” approach of sequence alignment: we first choose a single “seed” pair of nodes (one node from each network) with high topological similarity. We then expand the alignment radially outward around the seed as far as practical using a greedy algorithm. Although local in nature, our algorithm produces large and dense global alignments. By “dense” we mean that the aligned subgraphs share many edges, which would not be the case in a low-quality or random alignment. We believe that the high quality of our alignments is based less on the details of the extension algorithm, and more on having a good measure of pair-wise topological similarity between nodes.<sup>34</sup>

To judge the statistical significance of our alignment, we first compare it to random alignments without regard to biological significance. Given a random alignment of yeast2 to human1, the probability of obtaining an edge correctness of 10.06% or better ( $p$ -value) is less than  $7 \times 10^{-8}$ ; the probability of obtaining a large CCS would be significantly smaller, so this represents a weak upper bound on our  $p$ -value. Our alignment also suggests that yeast2 and human1 share more topological similarity than would be expected for two random networks of the same size and similar structure. In particular, if we align networks drawn from several different random graph models<sup>35</sup> that have the same number of nodes and edges as yeast2 and human1, then the edge correctness between random networks is significantly lower than the edge correctness of our yeast2-human1 alignment. For example, aligning two Erdős-Rényi random graphs with the same degree distribution as the data gives an edge correctness of only about 4.8–0.5%. Similar alignments of Barabási-Albert type scale-free networks,<sup>36</sup> stickiness model networks,<sup>37</sup> or 3-dimensional geometric random graphs,<sup>38</sup> give edge correctness scores of only 3.3–0.3%, 5.9–0.3% and 7.2–0.4%, respectively. Arguably the best currently known model for PPI networks is the geometric graph model.<sup>37–40</sup> Using this as our null model, the  $p$ -value of our yeast2-human1 alignment is at most 0.05, suggesting that the yeast and human PPI networks

share topological similarities that are due to more than just chance.

In regards to our phylogenetic trees, note that since some of the pathways in KEGG are experimentally determined while others are determined partly by genetic sequence comparison, our results are not entirely independent of sequence; this will be rectified as the KEGG database is updated in the future to have metabolic pathways that are determined solely by experiment. At that time, our phylogenetic trees will provide a new and completely independent, objective source of phylogenetic information.

We note that optimal global alignments are not necessarily unique. Given any particular cost function, there may be many distinct alignments that all share the optimal cost. In this paper, we analyze just one specific alignment that we believe is good, although it may not be optimal according to our measure. Enumerating all optimal (or at least good) alignments requires extending our algorithm to allow many-to-many mappings between the nodes in the two networks. Thus, many more predictions of equal validity to those in this paper are likely to be possible.

The software and data used in this paper are available on request.

## References

- [1] Sharan, R. & Ideker, T. Modeling cellular machinery through biological network comparison. *Nature Biotechnology* **24**, 427–433 (2006).
- [2] Kelley, B. P. *et al.* PathBLAST: a tool for alignment of protein interaction networks. *Nucl. Acids Res.* **32**, W83–W88 (2004).
- [3] Berg, J. & Lassig, M. Local graph alignment and motif search in biological networks. *PNAS* **101**, 14689–14694 (2004).
- [4] Flannick, J., Novak, A., Balaji, S., Harley, H. & Batzoglou, S. Graemlin general and robust alignment of multiple large interaction networks. *Genome Res* **16**, 1169–1181 (2006).
- [5] Liang, Z., Xu, M., Teng, M. & Niu, L. NetAlign: a web-based tool for comparison of protein interaction networks. *Bioinformatics* **22**, 2175–2177 (2006).
- [6] Flannick, J., Novak, A. F., Do, C. B., Srinivasan, B. S. & Batzoglou, S. Automatic parameter learning for multiple network alignment. In *RECOMB*, 214–231 (2008).
- [7] Singh, R., Xu, J. & Berger, B. Pairwise global alignment of protein interaction networks by matching neighborhood topology. In *Research in Computational Molecular Biology*, 16–31 (Springer, 2007).
- [8] Radivojac, P. *et al.* An integrated approach to inferring gene-disease associations in humans. *Proteins* **72**, 1030–1037 (2008).

- [9] Collins, S. *et al.* Toward a comprehensive atlas of the physical interactome of *saccharomyces cerevisiae*. *Molecular and Cellular Proteomics* **6**, 439–450 (2008).
- [10] Stark, C. *et al.* BioGRID: A general repository for interaction datasets. *Nucleic Acids Research* **34**, D535–D539 (2006).
- [11] Peri, S. *et al.* Human protein reference database as a discovery resource for proteomics. *Nucleic Acids Res* **32 Database issue**, D497–501 (2004).
- [12] Rual, J. *et al.* Towards a proteome-scale map of the human protein-protein interaction network. *Nature* **437**, 1173–78 (2005).
- [13] Steinmetz, L. *et al.* Systematic screen for human disease genes in yeast. *Nature Genetics* **31**, 400–4 (2002).
- [14] Martinez, M. A. *et al.* Genetic analysis of three genes causing isolated methylmalonic acidemia: identification of 21 novel allelic variants. *Mol Genet Metab* **84**, 317–25 (2005).
- [15] Yang, X. *et al.* Mutation analysis of the MMAA and MMAB genes in Japanese patients with vitamin B(12)-responsive methylmalonic acidemia: identification of a prevalent MMAA mutation. *Mol Genet Metab* **82**, 329–33 (2004).
- [16] Hsieh, S. Y. *et al.* Comparative proteomic studies on the pathogenesis of human ulcerative colitis. *Proteomics* **6**, 5322–31 (2006).
- [17] Carlsson, H., Petersson, S. & Enerback, C. Cluster analysis of s100 gene expression and genes correlating to psoriasin (s100a7) expression at different stages of breast cancer development. *Int J Oncol* **27**, 1473–81 (2005).
- [18] Yuasa, T., Yoshiki, T., Isono, T., Tanaka, T. & Okada, Y. Molecular cloning and expression of uroplakins in transitional cell carcinoma. *Adv Exp Med Biol* **539**, 33–46 (2003).
- [19] Zhou, W. *et al.* Functional evidence for a nasopharyngeal carcinoma-related gene *bcat1* located at 12p12. *Oncol Res* **16**, 405–413 (2007).
- [20] Cherry, J. *et al.* SGD: *Saccharomyces Genome Database*. *Nucleic Acids Research* **26**, 73–79 (1998).
- [21] Green Kunz, J., Loeschmann, A., Deuter-Reinhard, M. & Hall, M. Fap1, a homologue of human transcription factor *nf-x1*, competes with rapamycin for binding to *fkbp12* in yeast. *Mol Microbiol.* **37**, 1480–93 (2000).
- [22] Garca-Rubio, M. *et al.* Different physiological relevance of yeast *tho/trex* subunits in gene expression and genome integrity. *Mol Genet Genomics* **279**, 123–32 (2008).



- [23] Lelivelt, M. & Culbertson, M. Yeast upf proteins required for rna surveillance affect global expression of the yeast transcriptome. *Mol Cell Biol.* **19**, 6710–9 (1999).
- [24] Labarga, A., Valentin, F., Andersson, M. & Lopez, R. Web services at the european bioinformatics institute. *Nucleic Acids Research* **35**, W6–W11 (2007).
- [25] Rost, B. Twilight zone of protein sequence alignments. *Protein Engineering* **12**, 85–94 (1999).
- [26] Suthram, S., Sittler, T. & Ideker, T. The plasmodium protein network diverges from those of other eukaryotes. *Nature* **438**, 108–112 (2005).
- [27] Agrafioti, I. *et al.* Comparative analysis of the saccharomyces cerevisiae and caenorhabdits elegans protein interaction networks. *BMC Evolutionary Biology* **5** (2005).
- [28] Kanehisa, M. & Goto, S. Kegg: Kyoto encyclopedia of genes and genomes. *Nucleic Acids Res.* **28**, 27–30 (2000).
- [29] Pennisi, E. Modernizing the tree of life. *Science* **300**, 1692 – 1697 (2003).
- [30] Keeling, P., Luker, M. & Palmer, J. Evidence from beta-tubulin phylogeny that microsporidia evolved from within the fungi. *Mol. Biol. Evol.* **17**, 23–31 (2000).
- [31] Tanriverdi, S. & Widmer, G. Differential evolution of repetitive sequences in cryptosporidium parvum and cryptosporidium hominis. *Infect. Genet. Evol.* **6**, 113–22 (2006).
- [32] Xu, P. *et al.* The genome of cryptosporidium hominis. *Nature* **431**, 1107–12 (2004).
- [33] Out, H. & Sayood, K. A new sequence distance measure for phylogenetic tree construction. *Bioinformatics* **19**, 2122–2130 (2003).
- [34] Milenković, T. & Pržulj, N. Uncovering biological network function via graphlet degree signatures. *Cancer Informatics* **4**, 257–273 (2008).
- [35] Milenković, T., Lai, J. & Pržulj, N. Graphcrunch: a tool for large network analyses. *BMC Bioinformatics* **9** (2008).
- [36] Barabási, A. & Albert, R. Emergence of scaling in random networks. *Science* **286**, 509–512 (1999).
- [37] Pržulj, N. & Higham, D. Modelling protein-protein interaction networks via a stickiness index. *Journal of the Royal Society Interface* **3**, 711–716 (2006).
- [38] Pržulj, N., Corneil, D. G. & Jurisica, I. Modeling interactome: Scale-free or geometric? *Bioinformatics* **20**, 3508–3515 (2004).

Protein	Prediction	Pubmed ID
A1BG	binding	15461460
A1BG	regulation of cell growth	17170084
PRCC	RNA splicing	11313942
IFIT2	transport	17030862
UBL5	transport	15620657, 15289900
GDNF	DNA-dependent DNA replication	16837611
GDNF	deoxiribonucleotide biosynthesis	16837611
FANCF	transcription corepressor activity	16784902
ING1	binding	15743678, 16893883
MKRN1	oxidoreductase activity	16785614
DENR	binding	17878526
ETV3	transcription	18025162
IFIT5	mRNA processing	17879257

Table 1: Literature-validated predictions for human proteins.

- [39] Pržulj, N. Biological network comparison using graphlet degree distribution. *Bioinformatics* **23**, e177–e183 (2006).
- [40] Higham, D., Rasajski, M. & Pržulj, N. Fitting a geometric graph to a protein-protein interaction network. *Bioinformatics* **24**, 1093–1099 (2008).
- [41] Hillis, D. M., Zwickl, D. & Guttel, R. Tree of life. University of Texas.

**Acknowledgments** We thank M. Rašajski for computational assistance. This project was supported by an NSF CAREER grant.

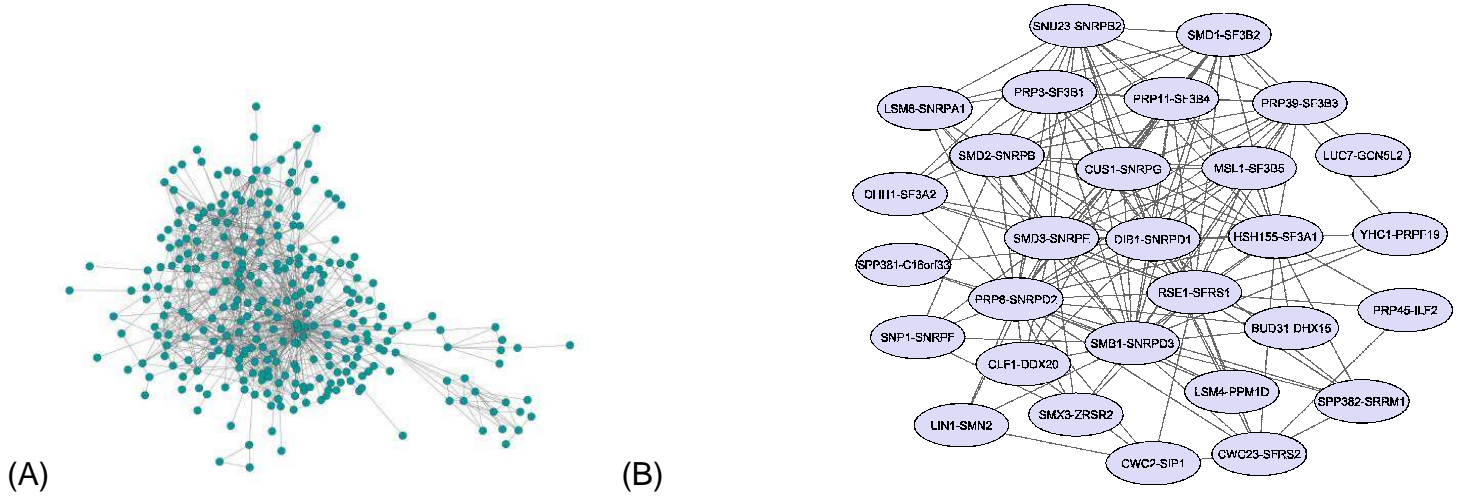


Figure 1: The alignment of yeast2 and human1 PPI networks. An edge between two nodes means that an interaction exists in both species between the corresponding protein pairs. Thus the displayed networks appear, in their entirety, in the PPI networks of both species. (A) The largest *common connected subgraph* (CCS) consisting of 1,001 interactions amongst 290 proteins. (B) The second largest CCS consisting of 157 interactions amongst 29 proteins. This subgraph has the same biological function (splicing) in both yeast2 and human1 PPI networks. Each node contains a label denoting a pair of yeast and human proteins that are aligned.

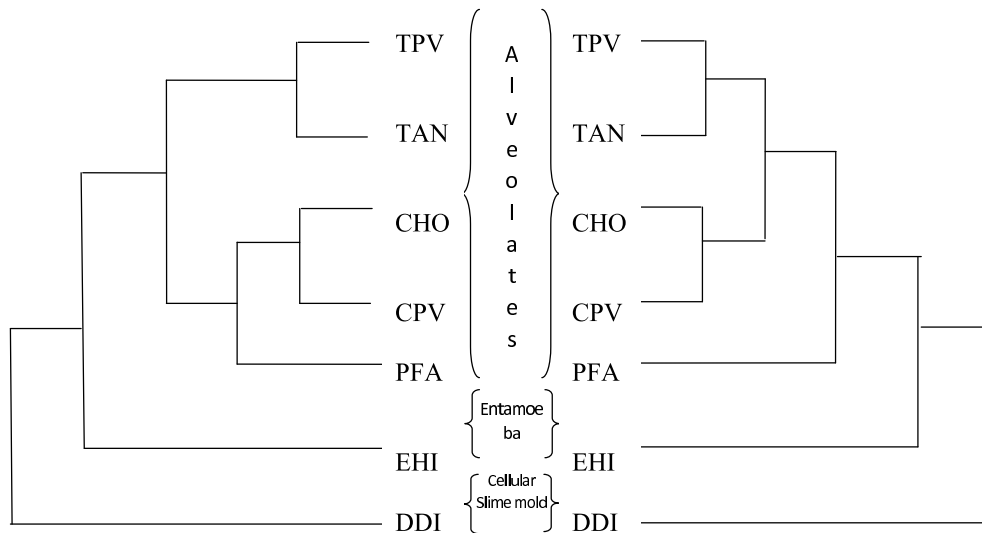


Figure 2: Phylogenetic tree for protists. Left: The tree obtained from genetic comparison.<sup>29,41</sup> Right: The tree produced by our algorithm. The following abbreviations are used for species: CHO - *Cryptosporidium hominis*, DDI - *Dictyostelium discoideum*, CPV - *Cryptosporidium parvum*, PFA - *Plasmodium falciparum*, EHI - *Entamoeba histolytica*, TAN - *Theileria annulata*, TPV - *Theileria parva*. The species are grouped into the following classes: "Alveolates", "Entamoeba", and "Cellular Slime mold".